

doi:10.15199/48.2023.09.28

Comparative performance analysis of variable speed controllers in a wind energy system using NARMA L2 neuro-controller and Super-twisting sliding mode controller

Abstract. Wind turbine performance is affected by wind speed, which can cause fluctuations in the frequency and voltage levels of the grid, leading to blackouts. To preserve grid stability, it is important to regulate wind turbine speed. In this paper, a comparative study of a super-twisting sliding mode controller and a NARMA L2 neuro-controller is implemented to control variable speed in a wind generator system, regarding their overshoot value, settling time, and rise time. The proposed controller's performance has been verified in MATLAB@Simulink. The simulation results indicate the greater performance of the NARMA-L2 neuro-controller in terms of robustness and the fastest dynamic response.

Streszczenie. Na wydajność turbiny wiatrowej wpływa prędkość wiatru, która może powodować wahania częstotliwości i napięcia w sieci, co prowadzi do przerw w dostawie prądu. Aby zachować stabilność sieci, ważne jest, aby regulować prędkość turbiny wiatrowej. W niniejszej pracy przeprowadzono analizę porównawczą super-skrętnego regulatora trybu ślizgowego i neuro-kontrolera NARMA L2 do sterowania zmienną prędkością w systemie generatora wiatrowego, w odniesieniu do ich wartości przekroczenia, czasu ustalania i czasu narastania. Działanie proponowanego regulatora zostało zweryfikowane w programie MATLAB@Simulink. Wyniki symulacji wskazują na większą wydajność neurosterownika NARMA-L2 w zakresie odporności i najszybszej odpowiedzi dynamicznej. (Analiza porównawcza wydajności regulatorów zmiennej prędkości w systemie energetyki wiatrowej z wykorzystaniem neurokontrolera NARMA L2 i kontrolera trybu ślizgowego Super-skręcanie)

Keywords: turbine model, speed control, NARMA L2, super-twisting sliding mode.

Słowa kluczowe: model turbiny, regulacja prędkości obrotowej, NARMA L2, tryb ślizgowy z super skrętem.

Introduction

Wind speed is a relevant parameter in wind power generation. Moreover, factors like static stability, shear, and turbulence in the atmosphere affect power energy [1]

As well, due to the unpredictability and quick fluctuations in wind speed, it can be difficult to integrate significant amounts of wind energy into an established grid system. This makes controlling wind energy quite challenging. Given that the instantaneous power output and consumption values are not equal, the result is a frequency deviation. [2] If somehow the wind energy produced is uncontrollable, the load will be damaged. [3] Sensitive electrical equipment can be affected by sudden voltage fluctuations. Even a single turbine might cause flicker in a vulnerable grid. [3] Keeping the voltage within the operational limit is always seen as one of the most important issues, particularly when integrating new technology connected to the load or power generation. For instance, depending on the variation in wind speed and type of generators, the fluctuation in wind power output results in voltage fluctuations and flickers. [4]

Using a variety of operating techniques, the grid operators have been capable of controlling the fluctuation by balancing the load with the available energy generation. In order to balance production and load, engineers shall immediately control the frequency of the grid within overly strict parameters [3].

The control of wind turbines is a topic of study for several researchers, such as [5] presented by applying nonlinear feedback controllers. The objectives are to synthesize robust controllers that maximize the energy extracted from the wind while reducing mechanical loads. [6]: A PID controller is employed for turbine rotor speed control and hence the frequency regulation. [7]: applied adaptive neuro-fuzzy inference system that is designed to estimate effective wind speed in real time using instantaneous values of mechanical power, rotor speed, and tip speed ratio for wind turbines. [8]: In order to achieve asymptotic and smooth rotor speed tracking, nonlinear and adaptive control techniques are utilized to modify the

excitation winding voltage of a wind turbine. [9]: proposes a basic fuzzy logic controlled inverter system for grid side inverter system control.

Nonlinear super-twisting sliding mode methods are currently a viable choice for the speed control of wind energy system such as [10]

The speed sensors in the control system models may end up being perfectly replaced by ANNs. [11] To build an effective system and minimize disturbance, the super twisting sliding mode and NARMA L2 controllers are supervised to reduce the peak overshoot as well as less rising and settling time.

Our research focused on achieving accurate wind turbine speed control using a super-twisting sliding mode Controller and a NARMA -L2 Controller. The main objective of this paper is to compare the rotor speed behavior of wind turbines using different control strategies, such as the conventional PID controller, the neural network controller (NARMA-L2), and the super-twisting sliding mode controller.

Modelling of wind turbine energy system

Wind turbines convert mechanical energy produced by the wind to electrical energy. The mechanical power transferred from the wind to the aerodynamic rotor is [12]

$$(1) \quad P_a = 0.5 \times \pi \times \rho \times R^2 \times [C_p(\lambda, \beta)] \times v_w^3$$

Where, C_p is the coefficient of power, ρ is the density of air, λ is the tip-speed ratio, β is the pitch-angle, R is the radius of the wind wheel, v_w is the wind speed. It is clear that the aerodynamic power P_a is directly proportional to the cube of the wind speed.

The relation between wind turbine's electromagnetic torque and rotor speed is defined as given in (2). [13-14]

$$(2) \quad T_{em} = T_l + J \frac{d\omega(t)}{dt} + F\omega(t)$$

Where, $\omega(t)$ is the rotor speed of wind turbine, T_{em} and T_l are the electromagnetic torque, the load one.

The complete transfer function of the wind turbine energy system is obtained by multiplying the sub transfer functions

of a mechanical model, a PMSG model and the boost dc-dc converter's as follows: [13-14]

$$(3) \quad G_T = (G_m) \times (G_p) \times (G_b)$$

$$= \left(\frac{1}{Js + F} \right) \times \left(\frac{\lambda P}{Z + R_s + L_s s} \right) \times \left(\frac{(1+d)V_0 - LI_i}{V_0 C_s + 2(1-d)I_i} \right)$$

$$G_T = \frac{1693.32}{0.000631s^3 + 4.499s^2 + 254.465s + 11.5573}$$

Where: G_m is the transfer function of the mechanical model, G_p is the transfer function of the permanent magnet synchronous generator (PMSG), G_b is the boost dc-dc converter's transfer function. It can be achieved by using the system values listed in Table 1. [14]

Table.1 wind turbine generator modelling values.

Parameter	Signification	Values
J	inertia	0.11kgm ²
F	Total friction	0.05N
λ	Tip speed ratio	0.07
p	The pair poles	8
d	Duty cycle	0.8
R_s	Resistance stator	0.3 Ω
L_s	Inductance stator	0.174mH
R_L	Load resistance	10 Ω
L	Boost inductance	4mH
V_0	Output voltage	50 V
I_i	Input current	24 A

PID controller

PID (Proportional-Integral-Derivative) controller is a feedback control loop mechanism used to regulate a system's output by adjusting its input. [15]. The PID controller variables essentially consist of three distinct variables: proportionality (k_p), quintessential (k_i), and spinoff values (k_d)

$$(4) \quad U_c(s) = \left[K_p + \frac{K_i}{s} + K_d s \right] E(s)$$

For a wind turbine speed controller, a PID controller block has been implemented in Simulink-MATLAB. Where $K_p=0.0603$, $K_i=0.05028$ and $K_d=0$. Chien-Hrones Reswick (CHR) algorithm [14]

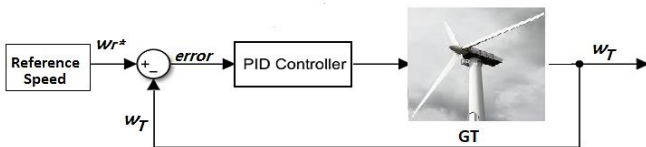


Fig.1.PID controller block diagram.

Super-twisting Sliding Mode Controller

SMC is an effective and efficient tool for solving nonlinear systems, robust to uncertainties, disturbances, and parameter variations. SMC has many applications in mechanical systems, but is limited when the relative degree of output is one, in addition to causing chattering due to its switching at a high frequency. the super-twisting sliding mode control (ST-SMC) has benefits such as lower effect on chattering, ability to reach equilibrium in finite time, and exact convergence while avoiding singularities. [16]

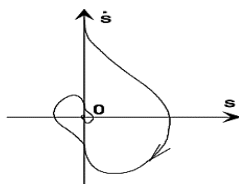


Fig.2. Convergence of the Super Twisting algorithm in the plane (S, \dot{S})

The trajectory of the super-twisting algorithm is considered as a spiral around the origin in the phase plane Fig. 2. The trajectory converges at the point of equilibrium (S, \dot{S}) in a finite time [16]. The sliding surface is chosen as the error on the quantity to be controlled in this case the speed of rotation of the turbine, where S is the tracking error:

$$(5) \quad S = \omega_{ref} - \omega_T$$

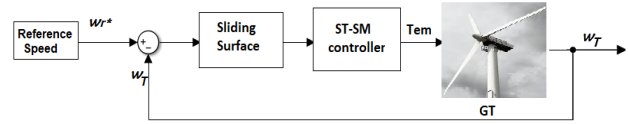


Fig.3. Super-twisting sliding mode control system

The sliding mode switching function for designing the super-twisting torque is given by the equation:

$$(6) \quad T_{em} = K_1 |S|^\alpha \text{sign}(s) + K_2 \int_0^t \text{sign}(s) d(t)$$

$\alpha=0.5$; Whereas $k_1, k_2 > 0$ are constant design parameters for sliding surface.

The ST-SM control law is presented by: [16]

$$(7) \quad u_{ST} = u_1(t) + u_2(t)$$

With:

$$(8) \quad \dot{u}_1 = -\delta_\omega \text{sing}(S_\omega)$$

$$u_2 = -\mu_\omega |S_\omega|^\eta \text{sing}(S_\omega) + u_1$$

the sliding surface, which is given as follows:

$$(9) \quad S_\omega = \omega_{ref} - \omega_T$$

Where δ_ω and μ_ω are positive constants, which are utilized to synthesize a robust ST-SM controller. The parameter η presents the degree of nonlinearity, which is generally defined as "0 < η \leq 0.5". This parameter is mostly equal to 0.5[17]

System stability proof

The stability is studied using the Lyapunov function:

$$(10) \quad V(S) = \frac{1}{2} S^2$$

Time derivative of equation (10):

$$(11) \quad \dot{V} = \dot{S} \cdot S(0)$$

The recommended controller is guaranteed to be globally asymptotically stable since the Lyapunov function's derivative is negative definite.

We can take sliding surface S as follows:

$$(12) \quad \text{sign}(s) = \begin{cases} 1 & \text{if } s > 0 \\ -1 & \text{if } s < 0 \end{cases}$$

Case 1:

For a higher reference speed than the measured speed $\omega_{ref} > \omega_T$, the speed control law is:

$$(13) \quad \omega_T = G_T \cdot T_{emref}$$

$$\dot{\omega}_T = s \cdot G_T \cdot T_{emref}$$

Where: ω_T is the speed turbine (velocity of the rotor), $\dot{\omega}_T$ is the derivative of the speed turbine, T_{emref} is reference torque, G_T transfer function of the wind turbine energy system

And:

$$(14) \quad s = \omega_{ref} - \omega_T > 0$$

In the following, the integral term is neglected.

Considering the sliding mode surface given by (14), the following expression can be written:

$$(15) \quad \begin{cases} \dot{\omega}_T = S.G_T.K_1 |S|^\alpha \text{sign}(s) + K_2 \int_0^t \text{sign}(s) d(t) \\ \dot{\omega}_T < 0 \quad \text{if } (S.G_T.K_1 |S|^\alpha \text{sign}(s)) < 0 \end{cases}$$

And:

$$(16) \quad \begin{cases} \dot{s} = -\text{Sign}(\dot{\omega}_T) \\ \dot{s} < 0 \end{cases}$$

It is clear from (14) and (16) the product is:

$$(17) \quad \dot{V} = \dot{S}.S < 0$$

Case 2:

For a higher measured speed than the reference speed

$\omega_{ref} < \omega_T$ so :

$$(18) \quad s = \omega_{ref} - \omega_T < 0$$

Using equation (18) we can re-write (19) as follows:

$$(19) \quad \begin{cases} \dot{\omega}_T = S.G_T.K_1 |S|^\alpha \text{sign}(s) + K_2 \int_0^t \text{sign}(s) d(t) \\ \dot{\omega}_T < 0 \quad \text{if } (S.G_T.K_1 |S|^\alpha \text{sign}(s)) < 0 \end{cases}$$

In this case:

$$(20) \quad \begin{cases} \dot{s} = -\text{Sign}(\dot{\omega}_T) \\ \dot{s} < 0 \end{cases}$$

So the Product (18)and (20)is: $\dot{V} = \dot{S}.S < 0$

In both cases:

$$(21) \quad \dot{V} = \dot{S}.S < 0$$

So the control is stable such that \dot{V} always remains negative definite.

Artificial neural network NARMA-L2 controller

The simple method for identifying a nonlinear discrete-time system is by using the Non-Linear Autoregressive Moving Average (NARMA) model. In a NARMA model the past, present input, and output values are used to determine future output values. The main concept of this controller is shifting of nonlinear system dynamic to a linear system by removal of nonlinearities in mapping. In NARMA-L2, a simple rearrangement of the neural network of the plant is to be controlled, which is trained offline [18].

This study describes the features of the NARMA-L2 controller and the speed control of the wind energy system that it implements. The diagram closed loop for controlling variable speed in wind turbine energy system with the NARMA L2 controller.

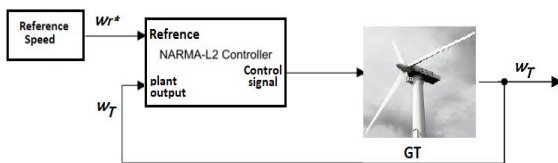


Fig .4. Artificial neural network control system.

There are two steps involved in NARMA-L2 controller which are [19]:

- Control design
- System identification

Control design

The NARMA-L2 controller consists of two multilayer neural networks (f) and (g) and two tapped delay lines (TDL) to store the values of input and output signals in the past. It maps the relationship between the input and output

using a linear structure consisting of weights and minimizes the weight equation iteratively until the optimal weight is achieved. Finally, it is tested on new input values. [18] The control law for this controller is:

$$(22) \quad u(k+1) = \frac{y_r(k+d) - [f(y(k), \dots, y(k-n+1), u(k-1), \dots, u(k-n+1))]}{g[y(k), \dots, y(k-n+1), u(k), \dots, u(k-n+1)]}$$

Where:

$$(23) \quad f = F[y(k), \dots, y(k-n+1), 0, u(k-1), \dots, u(k-n+1)]$$

$$(24) \quad g = \frac{\partial F}{\partial u(k)} [y(k), \dots, y(k-n+1), 0, u(k-1), \dots, u(k-n+1)]$$

Where u (k) and y (k) are the system input and output respectively [20]

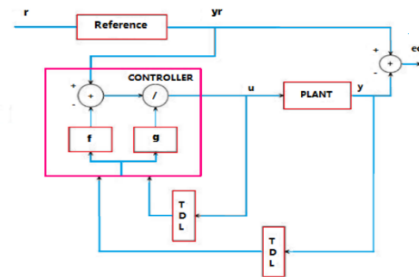


Fig.5. Diagram of NARMA L2 Controller. [20]

The identification of NARMA-L2 Controller

The first step in designing the NARMA-L2 neuro-controller is identifying the system that requires regulation.

In order to approximate the nonlinear function of f and g, the neuro-controller can be trained offline in batch using a group of input-output data pairs. [18]

Table.2: Identification plant of variable speed in wind turbine energy system of NARMA controller with all the adjusted parameter to generate data.

Network architecture	values
Size of hidden layer	8
Sampling Interval(sec)	0.03
Delayed plant input	3
Delayed plant Output	3
Training data	
Training samples	1000
Maximum plant input	1
Minimum plant input	0
Minimum plant output	0
Maximum plant output	1
Max interval value(sec)	5
Training parameters	
Training epochs	300

The NARMA-L2 neuro-controller is used to control the rotor speed of a wind turbine by determining the desired set point for the rotor speed, measuring the current rotor speed, designing a control signal to adjust the output, and implementing the controller on the wind turbine control system. Test and tune the controller to ensure it is accurately maintaining the desired rotor speed, and adjust the controller parameters to achieve the desired performance.

Results and discussion

The NARMA-L2 controller has been successfully modeled and tested to control the speed of wind turbines. The Levenberg-Marquardt back propagation algorithm has been used to train the controller. In order to generate data for the NARMA-L2 controller, it has been necessary to

generate the input and output data as a time series, where each input and output value is associated with a particular time step. Typically, the input data would be the past input and output values, and the output data would be the predicted future output value. This output will adjust the rotor speed to maintain the desired speed.

It has been noted that the quality of the training data will clarify the performance of the NARMA-L2 controller. After the data has been generated, it is shown in fig.6 as the plant input-output data of the NARMA-L2 controller.

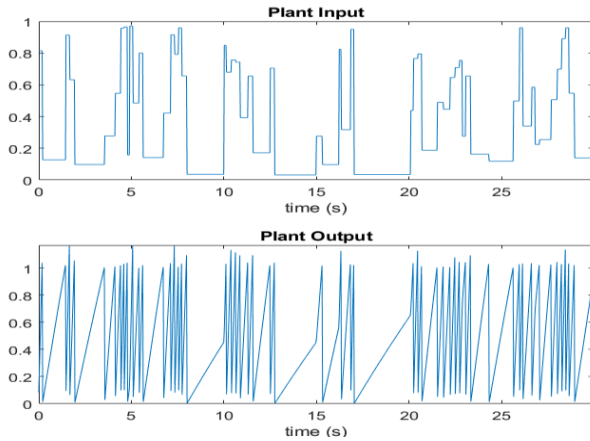


Fig.6. Plant input and output data of NN NARMA L2 controller.

Fig.7 shows the ANN model's mean square error. The mean square error (MSE) is used as performance, which decreases as the network's training progresses. The best validation performance is reached $8.0389e-11$ at epoch 201.

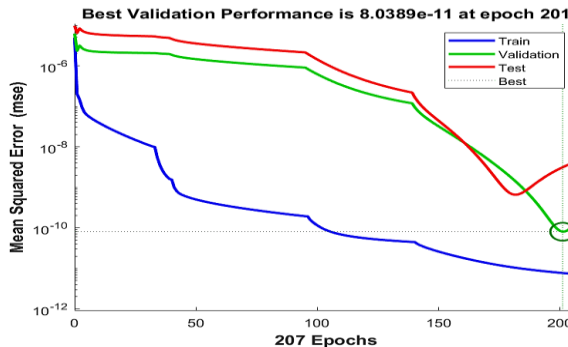


Fig.7. Neural network training performance.

In fig.8, it may be noted that regression is equal to 1, which means that ANN has successfully trained up to 100%. Furthermore, it may be noticed that the regression graph of the training set shows a good distribution of data in a straight line, showing that its training is complete. The training fitting is represented by the top left blue plot, the validation fitting is displayed on the top right green plot, then testing fitting is shown on the bottom left red plot, as well as the model fitting performance for all data sets is presented in the bottom right gray plot.

For controlling the rotor speed of the wind turbine, PID, NARMA-L2, and ST-SM controllers are successfully implemented in MATLAB/Simulink software. Fig. 9 presents the comparison of all proposed controllers. Simulation results for a set point of 1 (pu) show that the response of the PID controller comprises damped oscillations that die out at a time of 25.16 s. The settling time for a PID controller is 17.5833 seconds.

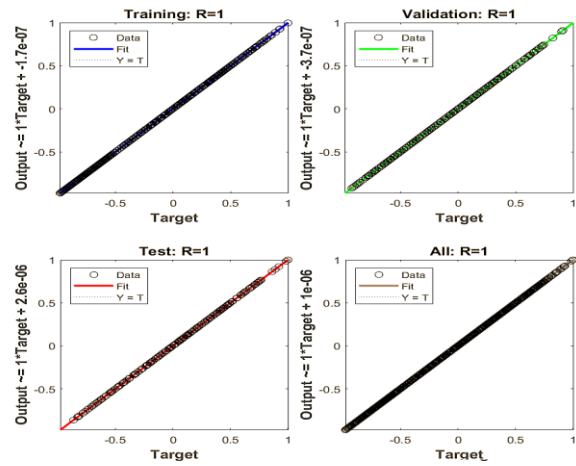


Fig.8. Neural network training regression.

After installing the neuro-controller and ST-SM controller, both controllers manage to follow the reference speed set by the controller; as well as the results of the ST-SM controller, it takes around 0.5128 s to readjust smoothly, whereas the NARMA-L2 controller takes 0.1785 s, which is less than the ST-SMC controller. Furthermore, the neuro-controller has the fastest rate of convergence compared to all other controllers. It can be seen that there is a negligibly small peak overshoot of 1.0078 (pu) in the case of NARMA-L2, while ST-SMC shows a lesser peak overshoot of 1.00185 (pu). However, it has a slower convergence rate than the neuro-controller.

The PID controller, on the other hand, is not as efficient as NARMA-L2 and ST-SMC, which show a significant overshoot of 1.3535 (pu). Furthermore, it has late convergence compared to NARMA-L2 and ST-SMC controllers.

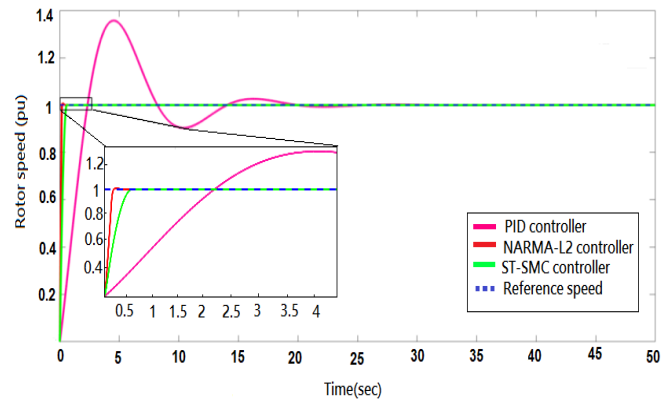


Fig.9: Response of NARMA L2, ST-SMC, PID of variable speed in wind turbine energy system.

The time domain response for speed regulation in wind turbine energy system equipped with the proposed controllers are detailed in table3.

Table.3: Comparison time domain response for speed reference with NARMA L2, ST-SMC, PID controllers

Speed controller	Rise time	Settling time	Peak time	Peak overshoot
NARMA L2	0.1240	0.1785	0.2931	1.0078
ST-SMC	0.3676	0.5108	0.6000	1.0018
PID	1.8046	17.5833	4.5354	1.3535

Table.3 illustrates the difference in the stabilization period between (NARMA L2, ST-SMC, and PID) responses, where Super-twisting sliding mode and NARMA L2 controllers provide better results than conventional PID controllers.

It can be observed that the ST-SMC controller gives superior results in terms of overshoot, rise time, and settling time than the conventional PID controller.

It has been noted that the NARMA L2 controller outperformed other regulators in terms of faster response presented by rise time; furthermore, in terms of settling time, it has the fastest rate of convergence compared to the ST-SMC and the PID controllers.

It can be concluded that the NARMA L2 controller is the most suitable strategy to be used in wind energy projects.

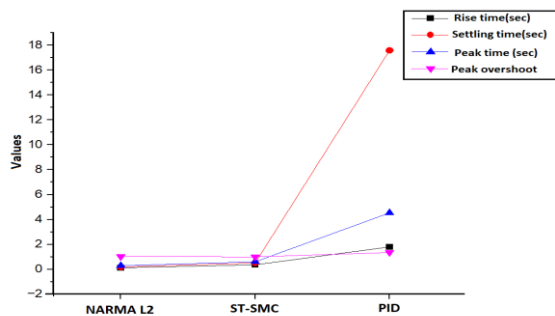


Fig. 10. The transient characteristics of the proposed controllers.

Conclusion

It is necessary to control the speed rotor of a wind turbine in order to keep the electrical grid's frequency constant because the electrical grid and a wind turbine's speed rotor are interdependent.

This paper compares different control strategies of variable speed in wind turbine energy systems.

The study of both the control ST-SMC controller and NARMA-L2 neuro-controller are more beneficial in providing fast rise time and faster system stabilization than the conventional PID control technique.

Compared to the ST-SMC controller and NARMA-L2 neuro-controller, the ANN produces the fastest response which there is only a small overshoot, and possesses good set-point tracking ability.

Finally, the use of ANNs is anticipated to increase soon as they are a viable solution for wind power systems.

Authors: M. Senouci, Ph.D. Student, Applied Power Electronics Laboratory (LEPA), Faculty of Electrical Engineering, Department of Electrotechnical Engineering University of Science and Technology of Oran Mohamed BOUDIAF, Algeria; E-mail: meriem.senouci@univ-usto.dz.

F. Benzergua, Prof.dr. University of Science and Technology of ORAN, Faculty of Electrical Engineering, Algeria, E-mail: benz_fad@yahoo.fr, N.Khalfallah Dr, Department of Electrical Engineering, National Polytechnic School of Oran-Maurice Audin (ENPO-MA), Algeria, E-mail: khalfalla_naima@yahoo.fr.

REFERENCES

[1] Sanchez Gomez, M., & Lundquist, J. K. (n.d.). *The effect of wind direction shear on turbine performance in a wind farm in central Iowa*. <https://doi.org/10.5194/wes-2019-22>

[2] Slootweg, J. G., & Kling, W. L. (2003). The impact of large scale wind power generation on power system oscillations. *Electric Power Systems Research*, 67(1), 9–20. [https://doi.org/10.1016/S0378-7796\(03\)00089-0](https://doi.org/10.1016/S0378-7796(03)00089-0)

[3] Liu, Y., & Zhang, J. (2018). Research on the effects of wind power grid to the distribution network of Henan province. *AIP Conference Proceedings*, 1955.

[4] Ahmed, S. D., Al-Ismael, F. S. M., Shafiullah, M., Al-Sulaiman, F. A., & El-Amin, I. M. (2020). Grid Integration Challenges of Wind Energy: A Review. In *IEEE Access* (Vol. 8, pp. 10857–10878). Institute of Electrical and Electronics Engineers Inc.

[5] Boukhezzar, B., & Siguerdidjane, H. (n.d.). Nonlinear Control of Variable Speed Wind Turbines without wind speed easurement. *Proceedings of the 44th IEEE Conference on Decision and Control*.

[6] Furat Abdal Rassul Abbas and Mohammed Abdulla Abdulsada. Simulation of Wind-Turbine Speed Control by MATLAB; *International Journal of Computer and Electrical Engineering*, Vol. 2, No. 5, October, 2010 1793-8163

[7] Asghar, A. B., & Liu, X. (2018). Adaptive neuro-fuzzy algorithm to estimate effective wind speed and optimal rotor speed for variable-speed wind turbine. *Neurocomputing*, 272, 495–504.

[8] Song, Y. D., Dhinakaran, B., & Bao, X. Y. (n.d.). *Variable speed Control of wind turbines using nonlinear and adaptive algorithms*.

[9] Muyeen, S. M., & Al-Durra, A. (2013). Modeling and control strategies of fuzzy logic controlled inverter system for grid interconnected variable speed wind generator. *IEEE Systems Journal*, 7(4), 817–824.

[10] Nasiri, M., Mobayen, S., & Zhu, Q. M. (2019). Super-Twisting Sliding Mode Control for Gearless PMSG-Based Wind Turbine. *Complexity*, 2019. <https://doi.org/10.1155/2019/6141607>

[11] Ahmed, S., Adil, H. M. M., Ahmad, I., Azeem, M. K., Huma, Z. E., & Khan, S. A. (2020). Super twisting sliding mode Algorithm based nonlinear MPPT control for a solar PV system with artificial neural networks based reference generation. *Energies*, 13(14).

[12] Doumi, M. H., Aissaoui, A., Tahour, A., Abid, M., & Tahir, K. (2016). Nonlinear integral backstepping control of wind energy Conversion system based on a Double – Fed Induction Generator. *Przeegląd Elektrotechniczny*, 92(3), 130-135.

[13] A. J. Mahdi, W. H. Tang, Q. H. Wu, "Derivation of a complete transfer function for a wind turbine generator system by experiments," in Proc. 2011 IEEE Power Engineering and Automation Conference, Vol. 1, pp. 35-38, 2011.

[14] R. Karthik, A. Sri Hari, Y. V. Pavan Kumar, D. John Pradeep "Modelling and Control Design for Variable Speed Wind Turbine Energy System". *2020 International Conference on Artificial Intelligence and Signal Processing (AISP) January 10-12, 2020, VIT-AP University, Amaravati, Andhra Pradesh, India- 52223*.

[15] Yang, C., Ren, E., & Dang, J. (2012). Analysis research of control method model on automobile brake test rig. *Przeegląd Elektrotechniczny*, 88(7b), 375-378.

[16] Al-Dujaili, A. Q., Falah, A., Humaidi, A. J., Pereira, D. A., & Ibraheem, I. K. (2020). Optimal super-twisting sliding mode Control design of robot manipulator: Design and comparison study. *International Journal of Advanced Robotic Systems*, 17(6).

[17] Dekali, Z., Baghli, L., & Boumediene, A. (2021). Improved Super twisting based high order direct power sliding mode Control of a connected dfig variable speed wind turbine. *Periodica Polytechnica Electrical Engineering and Computer Science*, 65(4), 352–372.

[18] Dash, S. (n.d.). *Load Frequency Control of Solar PV and Solar Thermal Integrated Micro grid using Narma-L2 Controller*

[19] Alhanjouri, M. (2015). Speed Control of DC Motor Using Artificial Neural Network. *International Journal of Science and Research*, 6, 2319–7064.

[20] Koleva, R., Lazarevska, A. M., & Babunski, D. (2022). Artificial Neural Network based Neuro controller for Hydropower Plant Control. *TEM Journal*, 11(2), 506 – 512